Photoluminescent Poly(*p*-phenylenevinylene)s with an Aromatic Oxadiazole Moiety as the Side Chain: Synthesis, Electrochemistry, and Spectroscopy Study

Zhi-Kuan Chen,† Hong Meng,† Yee-Hing Lai,‡ and Wei Huang*,†

Institute of Materials Research and Engineering and Department of Chemistry, National University of Singapore, Singapore 119260

Received December 4, 1998

ABSTRACT: Two poly(*p*-phenylenevinylene) (PPV) based polymers functionalized with an electron-deficient oxadiazole segment as the side chain by mimicking the chemical structure of 2-(4-biphenylyl)-5-(4-*tert*-butylphenyl)-1,3,4-oxadiazole (PBD) have been successfully synthesized through the Gilch route and Wittig method. The obtained polymer **II,** which is a copolymer, is completely soluble in conventional organic solvents. However, polymer **I**, which is a homopolymer, is not soluble in any common organic solvents tried. The structure and purity of **II** have been characterized by FT-IR, ^{1}H NMR, ^{13}C NMR, gel permeation chromatography (GPC), thermogravimetric analysis (TGA), differential scanning calorimetry (DSC), UV−vis and photoluminescence (PL) spectroscopy, and electrochemical analysis. The TGA results indicate that **II** has very high thermal stability, while DSC investigation demonstrates that the glass transition temperature (T_g) of **II** is higher than 200 °C, which might be a merit for the long-life operation of light-emitting devices. The absorption spectrum of film sample of **II** reveals two peaks, and the edge absorption corresponds to a band gap of 2.36 eV. The photoluminescence spectra indicate that this polymer is an orange-yellow emitting material. Electrochemical analysis through cyclic voltammetry demonstrates that this polymer is electroactive, showing reversible n-doping and p-dopable processes. The onset potential of reduction is comparable to that of PBD, which means the electron affinity of this polymer is readily enhanced by introducing an electron-withdrawing group as the side chain, and the situation of imbalance of charge injection ability could be improved. The HOMO and LUMO energy levels have also been estimated.

Introduction

Since the first report of polymeric light-emitting diodes (PLEDs) based on poly(*p*-phenylenevinylene) (PPV) by the Cambridge group,[1] great progress has been made in the study of PLEDs due to their promising application in the field of patterned light source and flat panel display. Much work has been done to develop novel luminescent polymeric materials with good processability, environmental stability, and intense luminance as well as to optimize the device structures to improve the efficiencies.[2−6] So far, several luminescent polymer systems have been established, for example, PPV and its derivatives,[1−3,7] poly(*p*-phenylene)s,[8,9] polythiophenes,[10,11] pyridyl-containing polymers,[12,13] polyfluorenes,[14−16] polycarbazoles,[17,18] etc.

It is believed that electroluminescence is generated from the radiative decay of singlet excitons which are produced by the recombination of the opposite charged carriers in the luminescent polymer layer in a sandwiched structured LED device. The opposite charges are separately injected from the two contacts under a bias voltage. The luminescent efficiency of the device is determined by the amount of charge carrier injection, the probability of the capture of the charges, and the ratio of the singlet excitons formed. It is known that most of the conjugated polymers used as light-emitting materials tend to be p-type polymers with much greater tendency for injecting and transporting holes than for electrons.[3] Therefore, the imbalance of rates for electron and hole injection from the negative and positive contacts becomes the obstacle for improving the electroluminescent efficiency. Although a low work function metal such as calcium or magnesium can be used as the cathode to lower the energy barrier so as to enhance the injection rate for electrons, the high chemical reactivity to oxygen and moisture of such metals limits their practicality. An alternative strategy by adding charge injection/transporting layers between the light-emitting polymer film and electrodes[19−21] or by blending the emission polymer with electron-transporting materials[22,23] has been widely used to improve the EL quantum efficiency of PLEDs. However, multilayer devices could cause a buildup of positive space charges and tunneling of accumulated holes thus damaging the devices,[24] while blend systems unavoidably encounter the problem of phase separation between the two different kinds of materials, which is caused by recrystallization or aggregate formation.[25] Consequently, design and synthesis of high electron affinity polymers, while keeping their hole injection ability and high emission properties, are challenging for materials chemists, and fortunately there is considerable room for optimization of the polymer optoelectronic properties through chemical modifications.[3,26,27] Indeed, a polymer with cyano substituents (CN−PPV) has demonstrated high electron affinity and has been successfully fabricated into a two-layered device with extremely high quantum efficiency (4%).[3]

In our previous work,[26−30] we have put forward a p−n diblock concept for the electroluminescent polymer design, in which the polymer is composed of a p-dopable block (e.g., an oligothiophene unit) and a n-dopable block (e.g., an aromatic oxadiazole moiety). On the basis of

* To whom correspondence should be addressed. E-mail: weihuang@imre.org.sg.
† Institute of Materials Research and Engineering.
‡ Department of Chemistry.

10.1021/ma981884y CCC: $18.00
Published on Web 06/10/1999

Scheme 1. Chemical Structures for Polymers I and II (EH Represents 2-Ethylhexyl)

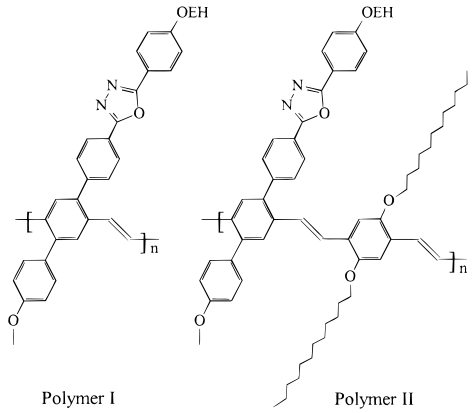

this idea, the intrinsic ability for balanced injection of electrons and holes is achieved. However, the oxadiazole unit inserted into the polymer backbone will partially act as the hole-blocking unit due to its high electron deficiency, which may lower the hole mobility in the device. Therefore, to further improve the charge-injecting and -transporting properties, we design a new homopolymer as well as a copolymer, in which the high electron affinity group of oxadiazole segment is introduced as the side chain into the PPV system. PPV derivatives have the advantages of facile processability to form thin films, morphological stability over a wide temperature range, and more versatility for synthesis. The molecular structures of the two polymers are displayed in Scheme 1. The structural design for one of the side chains is based on an idea to imitate the well-known electron-transporting material, 2-(4-biphenylyl)-5-(4-*tert*-butylphenyl)-1,3,4-oxadiazole (PBD), which can combine both the merits of PBD and PPV. As far as we know, the more aromatic rings the polymer structure contains, the easier the charge injection from the contacts for both the electrons and holes into the polymer will be, which can lower the turn-on voltage for the device operation as well as improve the quantum efficiency.[31] Hence, the other side chain is designed to be a *p*-methoxyphenylene ring. The asymmetric structure designed herein can also provide the polymer films with an amorphous property since asymmetry leads to the formation of configuration isomers of the repeat units along the polymer backbone and causes the decrease in crystallinity of the resulting polymers.[32] In addition, the bulk substitution with aromatic rings and electron-withdrawing oxadiazole-containing side chain on the phenylene ring also has a potential advantage of dispersing the electron atmosphere density on the vinylene segment so as to decrease the opportunity to be oxidized by oxygen.[33] The copolymer design is aimed at tuning the color and trying to obtain an orange or yellow light-emitting material as well as improving the processability through introducing two flexible long aliphatic chains on the other block. On the basis of this structure, a good solubility can be expected, and the fabrication process for the active emissive layer will be easy.

Experimental Section

Measurements. NMR spectra were collected on a Bruker ACF 300 spectrometer with chloroform-*d* as solvent and tetramethylsilane as internal standard. FT-IR spectra were recorded on a Bio-Rad FTS 165 spectrometer by dispersing

Scheme 2. Routes for Synthesis of Monomer I and Polymer I (EH Represents 2-Ethylhexyl)[a]

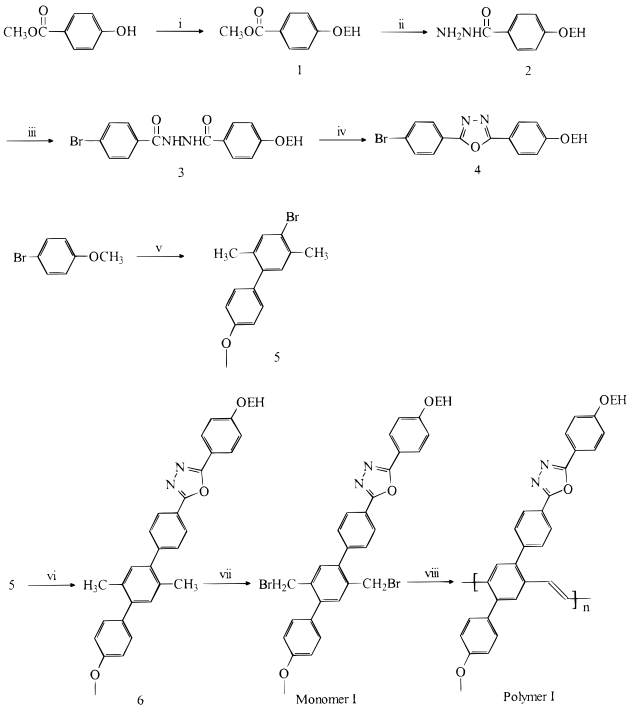

[a]Reagents and conditions: (i) 2-ethylhexyl bromide/K_2CO_3/acetone; (ii) $NH_2NH_2{\cdot}H_2O$/reflux; (iii) 4-bromobenzoyl chloride/TEA/CH_2Cl_2; (iv) $POCl_3$/reflux; (v) Mg/diethyl ether/2,5-dibromo-*p*-xylene/Ni(dppp)Cl_2; (vi) Mg/THF/**4**/Ni(dppp)Cl_2; (vii) NBS/benzene/BPO/$h\nu$; (viii) ^{t}BuOK/THF.

samples in KBr disks. UV−vis and fluorescence spectra were obtained on a Shimadzu UV−NIR 3100 spectrophotometer and on a Perkin-Elmer LS 50B luminescence spectrometer, respectively. Thermogravimetric analysis (TGA) was conducted on a DuPont Thermal Analyst 2100 system with a TGA 2950 thermogravimetric analyzer under a heating rate of 20 °C/min and a nitrogen or air flow rate of 75 mL/min. Differential scanning calorimetry (DSC) was run on a DuPont DSC 2910 module in conjunction with the DuPont Thermal Analyst system. Elemental microanalyses were performed on a Perkin-Elmer 240C elemental analyzer for C, H, N, and S determinations. Cyclic voltammetry (C−V) was performed on an EG&G Parc model 273A potentiostat/galvanostat system with a three-electrode cell in a solution of Bu_4NBF_4 (0.1 M) in acetonitrile at a scan rate of 20 mV/s. The polymer films were coated on a square Pt electrode (0.50 cm^2) by dipping the electrode into the corresponding solutions and then drying in air. A Pt wire was used as the counter electrode, and a $Ag/AgNO_3$ (0.1 M) electrode was used as the reference electrode. Prior to each series of measurements the cell was deoxygenated with argon. Gel permeation chromatography (GPC) analysis was conducted on a Perkin-Elmer model 200 HPLC system equipped with Phenogel MXL and MXM columns using polystyrene as standard and THF as eluent.

Materials. Diethyl ether was distilled over sodium/benzophenone. Hexane and chloroform were distilled over calcium hydride. Dry ethanol was obtained by distillation over magnesium. *N*,*N*-Dimethylformamide (DMF) was dried over 4 Å molecular sieves. 2-Ethylhexyl bromide, 1-bromododecane, 4-bromoanisole, hydroquinone, methyl 4-hydroxybenzoate, 2,5-dibromo-*p*-xylene, *N*-bromosuccinimide (NBS), dichloro-[1,3-bis(diphenylphosphino)propane]nickel(II) (Ni(dppp)Cl_2), triphenylphosphine, magnesium turnings, thionyl chloride, and phosphorus oxychloride were purchased from Aldrich and used without further purification.

Methyl 4-(2′-Ethylhexyloxy)benzoate (1). To a mixture of 50.0 g (0.33 mol) of methyl 4-hydroxybenzoate dissolved in 250 mL of acetone was added 55.2 g (0.40 mol) of potassium

Scheme 3. Routes for Synthesis of Monomers II and III and Polymer II (EH Represents 2-Ethylhexyl)[a]

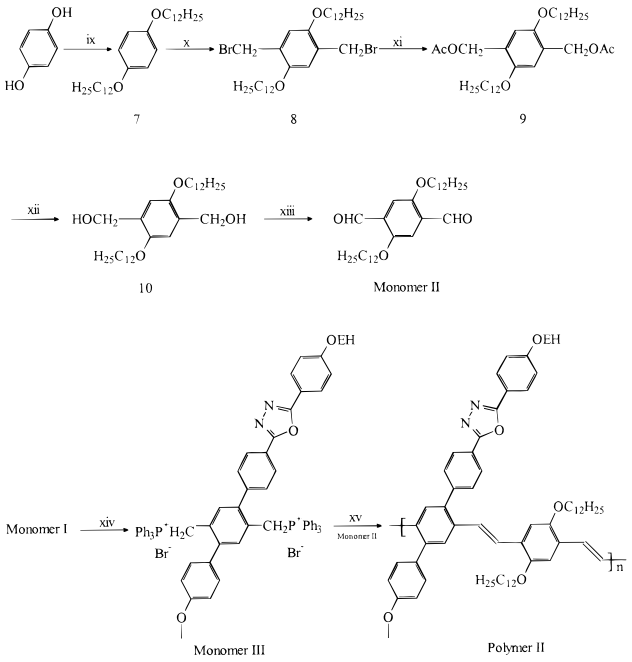

[a] Reagents and conditions: (ix) EtONa/EtOH/1-bromododecane; (x) $(CH_2O)_n$/HBr/AcOH; (xi) NaOAc/NaI/DMF; (xii) NaOH/EtOH/H_2O; (xiii) PCC/4 Å molecular sieves; (xiv) PPh_3/DMF; (xv) EtONa/EtOH/$CHCl_3$.

carbonate. The mixture was refluxed for 0.5 h, and then 77.2 g (0.40 mol) of 2-ethylhexyl bromide was added dropwise over a period of 1 h. The mixture was further refluxed for 48 h and then cooled and filtered. The solid thus obtained was washed with acetone. After the solvent of the combined filtrate was removed, the residue was dissolved in ethyl acetate and washed several times with 5% KOH and water and then dried with anhydrous magnesium sulfate. The solvent was removed by rotary evaporation, and the residue was distilled under reduced pressure (135 °C/0.2 mmHg) to afford a liquid product (61.1 g, yield 70%). MS: *m*/*z* 264. ^{1}H NMR ($CDCl_3$): δ 7.98−7.95 (d, J = 8.9, 2H), 6.91−6.88 (d, J = 8.9, 2H), 3.88−3.86 (d, J = 5.7, 2H), 3.86 (s, 3H), 1.74−1.68 (m, 1H), 1.52−1.28 (m, 8H), 0.94−0.87 (m, 6H) ppm.^{13}C NMR ($CDCl_3$): δ 166.74, 163.09, 131.42, 122.15, 113.98, 70.53, 51.81, 39.18, 30.36, 28.93, 23.70, 22.90, 13.93, 10.99 ppm. Anal. Calcd for $C_{16}H_{24}O_3$: C, 72.69; H, 9.15. Found: C, 72.77; H, 9.33.

4-(2′-Ethylhexyloxy)benzoylhydrazine (2). A mixture of 25.0 g (0.095 mol) of **1** and 15 g of excess hydrazine monohydrate was refluxed for 3 h. The reaction mixture was cooled and then recrystallized from ethanol. A white crystal product was obtained with a total amount of 23.0 g (yield 92%); mp 83.0−83.5 °C. MS: *m*/*z* 264. ^{1}H NMR ($CDCl_3$): δ 8.31−7.80 (b, NH, 1H), 7.74−7.71 (d, J = 8.7, 2H), 6.90−6.87 (d, J = 8.7, 2H), 4.3−3.7 (b, NH_2, 2H), 3.86−3.84 (d, J = 5.7, 2H), 1.75−1.67 (m, 1H), 1.53−1.27 (m, 8H), 0.93−0.86 (m, 6H) ppm.^{13}C NMR ($CDCl_3$): δ 168.30, 162.18, 126.69, 124.41, 114.26, 70.57, 39.16, 30.34, 28.94, 23.60, 22.90, 13.95, 10.87 ppm. Anal. Calcd for $C_{15}H_{24}N_2O_2$: C, 68.15; H, 9.15; N, 10.60. Found: C, 68.50; H, 9.03; N, 10.70.

1-(4′-Bromo-benzoyl)-2-(4′-(2″-ethylhexyloxy)benzoyl)-hydrazine (3). A 8.04 g (0.037 mol) sample of 4-bromobenzoyl chloride dissolved in 30 mL of CH_2Cl_2 was added into a solution containing 9.67 g (0.037 mol) of **2** and 3.74 g (0.037 mol) of triethylamine in 60 mL of CH_2Cl_2 under vigorous stirring. The reaction mixture was further stirred for 2 h and then extracted with water three times. The organic layer was dried over anhydrous $MgSO_4$. The solution was filtered and concentrated, and the resulting solid was recrystallized from ethanol/water to yield 15.4 g (94%) of white crystals; mp 166.5−167.5 °C. MS: *m*/*z* 447. ^{1}H NMR ($CDCl_3$): δ 10.71−10.70 (d, J = 3.5, NH, 1H), 10.21−10.20 (d, J = 3.4, NH, 1H), 7.76−7.73 (d, J = 8.8, 2H), 7.65−7.62 (d, J = 8.5, 2H), 7.38−7.35 (d, J = 8.6, 2H), 6.78−6.75 (d, J = 8.6, 2H), 3.84−3.82 (d, J = 5.7, 2H), 1.74−1.69 (m, 1H), 1.53−1.29 (m, 8H), 0.95−0.88 (m, 6H) ppm.^{13}C NMR ($CDCl_3$): δ 165.99, 165.16, 162.57, 131.40, 129.97, 129.34, 129.00, 126.78, 122.88, 114.07, 70.62, 39.15, 30.35, 28.95, 23.70, 22.93, 13.99, 11.00 ppm. Anal. Calcd for $C_{22}H_{27}BrN_2O_3$: C, 59.06; H, 6.08; Br, 17.86; N, 6.26. Found: C, 59.23; H, 5.98; Br, 17.61; N, 6.43.

2-(4-Bromophenyl)-5-(4-(2′-ethylhexyloxy)phenyl)-1,3,4-oxadiazole (4). A 10.0 g (0.022 mol) sample of **3** was refluxed in 40 mL of $POCl_3$ under nitrogen atmosphere for 8 h. After about 20 mL of $POCl_3$ was distilled off, the reaction mixture was cooled to 50 °C and then poured into 150 mL of ice water. The white precipitate obtained was collected by filtration and washed with water. A 9.6 g sample of white crystals was obtained by recrystallization from ethanol (yield 92%); mp 101.0−102.5 °C. MS: *m*/*z* 429. ^{1}H NMR ($CDCl_3$): δ 7.99−7.96 (d, J = 8.8, 2H), 7.92−7.89 (d, J = 8.5, 2H), 7.60−7.57 (d, J = 8.5, 2H), 6.98−6.95 (d, J = 8.8, 2H), 3.88−3.86 (d, J = 5.6, 2H), 1.72−1.70 (m, 1H), 1.52−1.30 (m, 8H), 0.94−0.89 (m, 6H) ppm.^{13}C NMR ($CDCl_3$): δ 164.59, 163.12, 162.18, 132.19, 128.52, 128.01, 125.95, 122.87, 115.68, 114.88, 70.65, 39.18, 30.35, 28.95, 23.71, 22.93, 13.99, 11.02 ppm. Anal. Calcd for $C_{22}H_{25}BrN_2O_2$: C, 61.54; H, 5.87; Br, 18.61; N, 6.52. Found: C, 61.63; H, 5.84; Br, 18.39; N, 6.72.

2-Bromo-5-(4-methoxyphenyl)-*p*-xylene (5). A Grignard reagent of anisole-4-magnesium bromide (0.10 mol), prepared from the reaction of 18.7 g (0.10 mol) of 4-bromoanisole with 2.6 g (0.11 mol) of Mg in 200 mL of dry ether, was added dropwise into a solution of 2,5-dibromo-*p*-xylene (25.0 g, 0.095 mol) in 250 mL of dry ether containing 0.438 g (0.8 mmol) of $Ni(dppp)Cl_2$ as catalyst over a period of 1.5 h. After refluxing for 20 h, the reaction mixture was quenched with 0.2 M HCl and extracted with ether. The extract was washed with water three times, with brine once, and then was dried over anhydrous Na_2SO_4. After removal of the solvent, a dark-brown liquid was obtained. The residue was subjected to purification by chromatography on silica gel using hexane/ethyl acetate (100:1) as eluent. The final product was further purified by distillation under reduced pressure (152 °C/0.4 mmHg) to give 17.5 g (yield 60%) of a white waxy solid. MS: *m*/*z* 291. ^{1}H NMR ($CDCl_3$): δ 7.46 (s, 1H), 7.25−7.22 (d, J = 8.7, 2H), 7.11 (s, 1H), 6.99−6.96 (d, J = 8.7, 2H), 3.87 (s, 3H), 2.41 (s, 3H), 2.24 (s, 3H) ppm.^{13}C NMR ($CDCl_3$): δ 158.53, 140.67, 134.84, 134.73, 133.60, 133.21, 132.06, 130.02, 123.07, 113.53, 55.21, 22.20, 19.70 ppm. Anal. Calcd for $C_{15}H_{15}BrO$: C, 61.87; H, 5.19; Br, 27.44. Found: C, 61.76; H, 5.13; Br, 27.33.

2-(4′-Methoxyphenyl)-5-{4′-[5″-(4‴-(2⁗-ethylhexyloxy)-phenyl)-1″,3″,4″-oxadiazole-2″-yl]phenyl}-*p*-xylene (6). The same procedure was used as described above for preparing compound **5**, except that diethyl ether was replaced by THF as the solvent. Thus, a Grignard reagent of 5-(4-methoxyphenyl)-*p*-xylene-2-magnesium bromide (0.02 mol), prepared from the reaction of 6.0 g (0.02 mol) of **5** with 0.6 g (0.025 mol) of Mg in 80 mL of THF, was added dropwise into a solution of **4** (8.0 g, 0.018 mol) in 150 mL of THF containing 88 mg (0.16 mmol) of $Ni(dppp)Cl_2$ as catalyst over a period of 1 h. After refluxing for 20 h, the reaction mixture was quenched with 0.2 M HCl and extracted with ether. The extract was washed with water three times, with brine once, and then was dried over anhydrous Na_2SO_4. After the solvent was removed, the residue was subjected to purification through silica gel chromatography using hexane/ethyl acetate (20:1) as eluent, followed by recrystallization from hexane to afford 4.6 g (yield 47%) of a white powder product; mp 114.5−116.0 °C. MS: *m*/*z* 560. ^{1}H NMR ($CDCl_3$): δ 8.20−8.17 (d, J = 8.4, 2H), 8.10−8.07 (d, J = 8.9, 2H), 7.56−7.53 (d, J = 8.4, 2H), 7.33−7.30 (d, J = 8.7, 2H), 7.18 (s, 2H), 7.06−7.03 (d, J = 8.9, 2H), 7.00−6.97 (d, J = 8.7, 2H), 3.95−3.93 (d, J = 5.7, 2H), 3.87 (s, 3H), 2.31 (s, 6H), 1.78−1.76 (m, 1H), 1.54−1.32 (m, 8H), 0.98−0.90 (m, 6H) ppm.^{13}C NMR ($CDCl_3$): δ 164.54, 164.02, 162.15, 158.56, 145.08, 141.05, 139.25, 133.77, 132.92, 132.34, 132.07, 131.49, 130.15, 129.65, 128.56, 126.54, 122.41, 116.07, 114.96, 113.48, 70.70, 55.20, 39.24, 30.41, 28.98, 23.75, 22.93, 19.90,

13.98, 11.02 ppm. Anal. Calcd for $C_{37}H_{40}N_2O_3$: C, 79.24; H, 7.19; N, 5.02. Found: C, 78.94; H, 7.25; N, 5.22.

2-(4′-Methoxyphenyl)-5-{4′-[5″-(4‴-(2⁗-ethylhexyloxy)-phenyl)-1″,3″,4″-oxadiazole-2″-yl]phenyl}-1,4-bis(bromomethyl)benzene (Monomer I). A 4.0 g (6.9 mmol) sample of **6,** 2.5 g (14.0 mmol) of NBS, and a catalytic amount of benzoyl peroxide (BPO) as an initiator were added into 50 mL of benzene. The reaction mixture was irradiated under a tungsten lamp and refluxed for 3 h under nitrogen atmosphere. The reaction mixture was washed with water three times, and then the organic layer was dried over anhydrous $MgSO_4$. The solution was filtered and concentrated, and the resulting solid was recrystallized from absolute ethanol to yield white crystals in 65% yield; mp 128.0−129.0 °C. MS: *m/z* 718. ^{1}H NMR ($CDCl_3$): δ 8.26−8.24 (d, J = 8.3, 2H), 8.11−8.08 (d, J = 8.6, 2H), 7.70−7.67 (d, J = 8.3, 2H), 7.46−7.43 (d, J = 9.1, 2H), 7.45 (s, 2H), 7.07−7.04 (d, J = 8.7, 2H), 7.04−7.01 (d, J = 8.5, 2H), 4.49 (s, 2H), 4.45 (s, 2H), 3.95−3.93 (d, J = 5.7, 2H), 3.89 (s, 3H), 1.80−1.74 (m, 1H), 1.60−1.34 (m, 8H), 0.98−0.90 (m, 6H) ppm.^{13}C NMR ($CDCl_3$): δ 164.68, 163.73, 162.21, 159.31, 142.51, 141.94, 140.11, 135.90, 135.35, 133.19, 132.66, 131.29, 130.01, 129.64, 128.61, 126.83, 123.46, 115.96, 114.98, 113.87, 70.72, 55.27, 39.24, 31.34, 30.98, 28.98, 23.76, 22.93, 13.97, 11.02 ppm. Anal. Calcd for $C_{37}H_{38}Br_2N_2O_3$: C, 61.85; H, 5.33; Br, 22.24; N, 3.90. Found: C, 61.51; H, 5.46; Br, 22.23; N, 3.99.

[2-(4′-Methoxyphenyl)-5-{4′-[5″-(4‴-(2⁗-ethylhexyloxy)phenyl)-1″,3″,4″-oxadiazole-2″-yl]phenyl}-1,4-xylylene]bis(triphenylphosphonium bromide) (Monomer III). A solution of 1.08 g (1.50 mmol) of monomer **I** and 0.869 g (3.30 mmol) of triphenylphosphine in 10 mL of DMF was heated to reflux for 24 h with stirring. The resulting mixture was poured into diethyl ether. The precipitate was filtered and recrystallized in ethanol−ethyl acetate to afford 1.45 g of white crystals; yield 78%, mp 265−267 °C. ^{1}H NMR ($CDCl_3$): δ 8.07−8.04 (d, J = 8.8, 2H), 7.91−7.88 (d, J = 8.3, 2H), 7.62−7.57 (m, 6H), 7.51−7.45 (m, 12H), 7.34−7.28 (m, 12H), 7.19−7.17 (d, J = 8.1, 2H), 7.04−7.01 (d, J = 8.9, 2H), 6.90 (s, 2H), 6.89−6.86 (d, J = 8.8, 2H), 6.72−6.69 (d, J = 8.6, 2H), 5.50 (s, 2H), 5.46 (s, 2H), 3.92−3.90 (d, J = 5.7, 2H), 3.78 (s, 3H), 1.74−1.72 (m, 1H), 1.51−1.30 (m, 8H), 0.94−0.86 (m, 6H) ppm.^{13}C NMR ($CDCl_3$): δ 164.78, 163.52, 162.28, 158.97, 142.63, 141.52, 140.63, 134.76, 134.71, 133.90, 133.81, 133.77, 130.39, 130.15, 130.07, 129.98, 128.63, 126.92, 122.94, 117.61, 117.38, 116.61, 115.72, 114.05, 70.72, 55.24, 39.20, 33.70, 30.36, 28.94, 23.71, 22.88, 13.93, 10.99 ppm. Anal. Calcd for $C_{73}H_{68}Br_2N_2P_2O_3$: C, 70.53; H, 5.51; N, 2.25. Found: C, 68.43; H, 5.78; N, 2.08.

1,4-Didodecyloxybenzene (7). Sodium ethoxide was prepared by adding 2.53 g (110 mmol) of sodium into 50 mL of anhydrous ethanol. After all the sodium disappeared, 5.5 g (50 mmol) of hydroquinone in 10 mL of anhydrous ethanol was added dropwise. To the stirred mixture, 28.0 g (112 mmol) of dodecyl bromide in 10 mL of anhydrous ethanol was added. After stirring for 24 h with refluxing, the ethanol was evaporated at reduced pressure. The brownish residue was added into 300 mL of water, extracted with ethyl acetate, and dried with anhydrous magnesium sulfate. The white product (21.0 g, yield 94%) was obtained by crystallization after most of the solvent was removed under reduced pressure; mp 74.5−75.5 °C. MS: *m/z* 446. ^{1}H NMR ($CDCl_3$): δ 6.81 (s, 4H), 3.91−3.87 (t, J = 6.6, 4H), 1.79−1.69 (m, 4H), 1.43−1.26 (m, 36H), 0.90−0.86 (t, 6H) ppm.

2.5-Didodecyloxy-1,4-bisbromomethylbenzene (8). A mixture of 4.46 g (10 mmol) of 1,4-didodecyloxybenzene and 1.28 g of paraformaldehyde in 15 mL of 46% hydrogen bromide in acetic acid was refluxed for 24 h. The mixture was poured into water and neutralized with saturated sodium carbonate. The precipitate was filtered and washed with water. The pure product was obtained by recrystallization in ethyl acetate to afford 4.2 g of white crystals with a yield of 66%; mp 96.0−97.0 °C. MS: *m/z* 632. ^{1}H NMR ($CDCl_3$): δ 6.85 (s, 2H), 4.52 (s, 4H), 4.00−3.96 (t, J = 6.4, 4H), 1.85−1.76 (m, 4H), 1.54−1.27 (m, 36H), 0.90−0.86 (t, 6H) ppm. Anal. Calcd for $C_{32}H_{56}Br_2O_2$: C, 60.76; H, 8.86; Br, 25.32. Found: C, 60.79; H, 8.69; Br, 25.30.

2,5-Didodecyloxy-1,4-phenylenemethylene diacetate (9). A 0.632 g (1.0 mmol) sample of **8**, 0.300 g (2.0 mmol) of sodium iodide, 0.492 g (6.0 mmol) of anhydrous sodium acetate, and 10 mL of DMF were charged in a 25 mL round-bottom flask. The mixture was heated to 140 °C through an oil bath and kept at this temperature for 2 days with stirring. After cooling to room temperature, the mixture was poured into 100 mL of water and extracted with ethyl acetate three times (25 mL each). The organic phase was washed with water and brine and then dried with anhydrous $MgSO_4$. After decolorization with active charcoal, the solvent was evaporated by rotary evaporation, and the residue was purified by recrystallization in ethyl acetate to afford 0.500 g of white crystals (yield 85%); mp 82.0−83.0 °C. MS: *m/z* 590. ^{1}H NMR ($CDCl_3$): δ 6.87 (s, 2H) 5.13 (s, 4H), 3.96−3.91 (t, J = 6.5, 4H), 2.09 (s, 6H), 1.78−1.73 (m,4H), 1.54−1.26 (m, 36H), 0.90−0.86 (t, 6H) ppm. Anal. Calcd for $C_{36}H_{62}O_6$: C, 73.18; H, 10.58. Found: C, 73.02; H, 10.86.

2,5-Didodecyloxy-1,4-bishydroxymethylbenzene (10). A 3.87 g (6.56 mmol) sample of diacetate compound **9** was added into 100 mL of mixed solvent of ethanol−water (1:1) containing 3.2 g of sodium hydroxide. The mixture was refluxed for 4 h with stirring. After cooling to room temperature, ethanol was evaporated through a rotary evaporator. The residue was extracted with ethyl acetate, and the organic layer was washed with water and brine and then dried by anhydrous $MgSO_4$. After the solvent was evaporated, the crude product was purified by recrystallization from ethyl acetate to give 3.14 g of white crystals (yield 95%); mp 108.5−110.0 °C. MS: *m/z* 506. ^{1}H NMR ($CDCl_3$): δ 6.85 (s, 2H), 4.68−4.66 (d, J = 5.5, 4H), 4.00−3.96 (t, J = 6.4, 4H), 2.38−2.33 (t, J = 5.4, 2H), 1.82−1.73 (m, 4H), 1.46−1.27 (m, 36H), 0.90−0.86 (t, 6H) ppm. Anal. Calcd for $C_{32}H_{58}O_4$: C, 75.84; H, 11.53. Found: C, 75.98; H, 11.76.

2,5-Didodecyloxy-1,4-diformylbenzene (Monomer II). A 3.36 g (6.0 mmol) sample of diol compound **10**, 5.25 g (24.0 mmol) of pyridium chlorochromate (PCC), 1.0 g of 4 Å freshly dried molecular sieves, 1.0 g of silicon gel, and 100 mL of dry methylene chloride were charged into a 150 mL round-bottom flask. The mixture was cooled to 0 °C in an ice bath and stirred for 4 h, warmed to room temperature, and stirred for another 24 h. TLC monitoring indicated the diol compound had been completely converted to diformyl product. The mixture was run through a reduced pressure silicon gel column (2.5 cm × 10 cm) eluted with hexane. After the solvent was evaporated, yellow crystals (3.32 g) were quantitatively obtained; mp 90.0−90.5 °C. MS: *m/z* 502. ^{1}H NMR ($CDCl_3$): δ 10.52 (s, 2H) 7.43 (s, 2H), 4.10−4.06 (t, J = 6.3, 4H), 1.85−1.81 (m, 4H), 1.52−1.27 (m, 36H), 0.90−0.86 (t, 6H) ppm. ^{13}C NMR ($CDCl_3$): δ 189.33, 155.14, 129.21, 111.55, 69.17, 63.54, 31.80, 29.53, 29.50, 29.46, 29.37, 29.20, 28.94, 25.90, 22.57, 13.99 ppm. Anal. Calcd for $C_{32}H_{54}O_4$: C, 76.45; H, 10.84. Found: C, 76.39; H, 10.78.

Polymer I, Method A. A solution of 0.300 g (0.42 mmol) of monomer **I** in 30 mL of anhydrous THF was charged in a 50 mL flask. To this stirred solution was added dropwise 1.7 mL of 1.0 M solution of potassium *tert*-butoxide (1.7 mmol) in anhydrous THF at room temperature. The mixture was stirred at ambient temperature for 2 h. The reaction mixture was then poured into 200 mL of methanol with stirring. The resulting yellow precipitate was washed with deionized water and dried under vacuum to afford 0.196 g (yield 84%) of a yellow powder. The polymer could not dissolve in any common organic solvents. FT-IR (KBr disk, cm^{-1}): 3037, 3001, 2956, 2927, 2857, 1611, 1586, 1497, 1484, 1464, 1441, 1426, 1381, 1300, 1250, 1173, 1100, 1067, 1030, 961, 903, 833, 739, 710, 658, 600, 542, 521. Anal. Calcd for $(C_{37}H_{36}N_2O_3)_n$: C, 79.83; H, 6.52; N, 5.03. Found: C, 75.06; H, 6.77; N, 4.82.

Polymer I, Method B. To a solution of 0.280 g (0.37 mmol) of monomer **I** in 30 mL of anhydrous *p*-xylene dried by sodium beads was added dropwise 1.1 mL of 1.0 M potassium *tert*-butoxide (1.1 mmol) in anhydrous THF solution at room temperature. Soon after the base was added, a light yellow-green precipitate appeared. The mixture was stirred for 1 h and then poured into 200 mL of methanol. The polymer powder

was collected and dried under vacuum. A 0.186 g sample of light yellow-green polymer was obtained. The as-synthesized polymer also could not dissolve in any common organic solvents.

Polymer II. A solution of 0.218 g (3.2 mmol) of sodium ethoxide in 10 mL of anhydrous ethanol was added to a stirred solution of 0.994 g (0.80 mmol) of triphenylphosphonium bromide monomer **III** and 0.402 g (0.80 mmol) of diformyl monomer **II** in 10 mL of anhydrous ethanol and 10 mL of dry chloroform. An orange precipitate was formed soon after the sodium ethoxide was added. The mixture was stirred for 10 h, and then it was poured into 200 mL of methanol. The orange polymer powder was collected by filtration and further purified by redissolving in chloroform and precipitating in methanol twice. After filtration and vacuum-drying, 0.474 g of polymer was obtained with a yield of 58%. ^{1}H NMR ($CDCl_3$): δ 8.28−7.87 (br, 4H), 7.87−7.61 (br, 1H), 7.61−7.30 (br, 4H), 7.25−7.10 (br, 2H), 7.10−6.95 (br, 4H), 6.95−6.71 (br, 4H), 6.68−6.39 (br, 1H), 3.89−3.75 (br, 6H), 3.53 (s, 3H), 1.64−1.16 (m, 52H), 0.94−0.85 (m, 9H). FT-IR (KBr disk, cm^{-1}): 3049, 3014, 2960, 2925, 2853, 1611, 1514, 1497, 1468, 1422, 1379, 1300, 1260, 1204, 1175, 1098, 1019, 833, 801, 722, 710, 660, 594, 544, 521. Anal. Calcd for $(C_{69}H_{90}N_2O_5)_n$: C, 80.66; H, 8.83; N, 2.73. Found: C, 78.93; H, 8.82; N, 2.54.

Results and Discussion

Polymer **I** is a PPV-based homopolymer, in which the side chain is composed of a *p*-methoxyphenyl group and an oxadiazole containing aromatic substituent with a long alkoxy chain. The structural design for the side chain is based on the idea of mimicking the well-known electron-transporting material of 2-(4-biphenylyl)-5-(4-*tert*-butylphenyl)-1,3,4-oxadiazole (PBD) aiming at improving the electron affinity of the polymer as described in the Introduction. The monomer is quickly polymerized in the potassium *tert*-butoxide−THF system, and a yellow polymer precipitate soon appeared. During the polymerization, intense yellow photoluminescence was observed even under the fluorescent lamp. However, the polymer could not be dissolved in any common organic solvents. To improve the processability of the designed polymer, more gentle polymerization conditions have been adopted, for example, to decrease the amount of base used, shorten the reaction time, and replace the more polar solvent such as THF with a less polar solvent such as *p*-xylene. Even under such conditions, the polymer obtained still could not be dissolved in any conventional organic solvents. The insolubility of the polymer might be caused by the suprarigid structure of the side chains, which is composed of several aromatic rings, such that the flexibility of the structure is lost to a high degree.

Polymer **II** is designed to improve the solubility by copolymerization with a block containing two long alkoxy side chains because of the relatively lowered rigidity of the polymer as well as the entropic contribution from the inserted block. In this structure, the charge transport can be achieved either through the polymer main chain or through the oxadiazole-containing side chains. Compared to dialkoxy substituted PPVs, the electron affinity can also be improved due to the existence of the oxadiazole moiety of the side chains. Indeed, the polymer obtained through the Wittig condensation reaction is completely soluble in chloroform, THF, xylene, toluene, dichloromethane, etc. Due to the good solubility of polymer **II**, the molecular weight measurement can be carried out by GPC. GPC analysis (polystyrene as the standard for calibration) reveals that the number-average molecular weight (M_n) and weight-average molecular weight (M_w) of the polymer are 12 600 and 31 100, respectively, with a polydispersity index of 2.47.

The purity of polymer **II** and corresponding monomers **I**, **II**, and **III** has been characterized through proton NMR. The NMR spectra are depicted in Figure 1. All the peaks' assignment here is based on the difference in chemical environments, the coupling constants, and reference to some compounds with similar structures synthesized in our lab. Figure 1A represents the spectrum of monomer **I**. It can be seen that protons on aromatic rings are clearly split and can be easily assigned. In the middle field region, the peaks from 4.49 to 3.89 ppm are assigned to bromomethyl groups, methyleneoxy in the long side chain, and the methoxy group, respectively. For monomer **II**, the spectrum is much simpler compared to that of monomer **I**. The three characteristic peaks at δ 10.51, 7.43, and 4.08 ppm are due to the resonance of protons on formyl group, phenylene ring, and alkoxy group, respectively. The ^{1}H NMR spectrum of monomer **III** is similar to that of monomer **I**. However, most of the aromatic protons shifted a little to the higher field due to the introduction of triphenyl phosphonium salt into the structure, while the doublets of $-CH_2-$ linked to the triphenyl phosphonium group shift to lower field at 5.48 ppm compared to the bromomethyl group in monomer **I**.

In Figure 1D, we can see that all the peaks of polymer **II** are much broader than those of the corresponding monomers, which is generally observed for polymer proton NMR. Since the spectrum is very complicated and broadened, the peak assignment becomes more difficult. It can be found that the characteristic peaks for the formyl proton of monomer **II** and methylene group linked to the triphenyl phosphonium group of monomer **III** disappeared completely, and a new peak at about 6.50 ppm appeared, which is the resonance of protons on the newly formed vinylene group. This result indicates that the Wittig reaction is rather successful and complete. It is well-known that the existence of the carbonyl group as well as any other impurities will quench the excitons when the material is used as the emission layer.[33] Only could a complete reaction of the formyl groups during the polymerization and successful purification after polymerization provide the possibility of high quantum efficiency when LED devices are fabricated utilizing this polymer as the emission layer.

Figure 2 demonstrates the thermogravimetric analysis (TGA) of the as-synthesized polymer **II**. The degradation pattern for the polymer in nitrogen is very simple. The polymer exhibits an onset for degradation at 386 °C, and no weight loss was observed at lower temperature. This onset temperature is higher than that of dialkoxy-substituted PPVs such as MEH−PPV or BEH−PPV (both onsets at 340 °C).[34] The maximum rate of weight loss takes place at 460 °C. Weight loss of 5 and 10% occurs at 421 and 434 °C, respectively. Above 650 °C, there is about 31 wt % of residue, which is produced by charring during heating. The result of TGA reveals that the polymer is quite stable in nitrogen. Figure 3 shows the DSC curve of polymer **II** at a heating rate of 20 °C/min under flowing nitrogen. The glass transition temperature (T_g) for the polymer is 205 °C. For PPV derivatives such as MEH−PPV or BEH−PPV, T_g is hardly observed.[34] However, the transition temperature observed here is higher than that of some other oxadiazole-containing small molecules or polymers.[19]

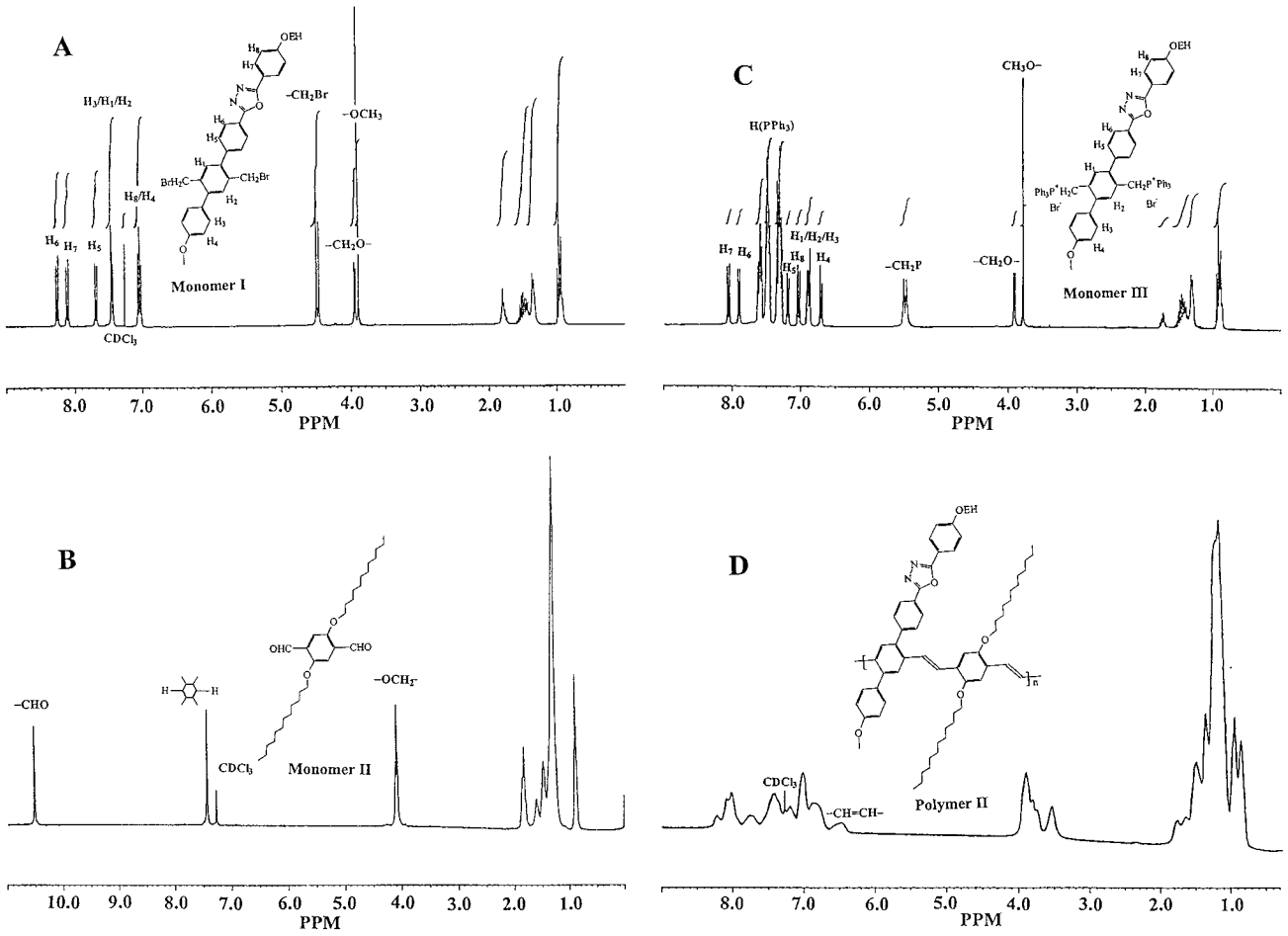

Figure 1. ^{1}H NMR spectra for monomers **I** to **III** and polymer **II**.

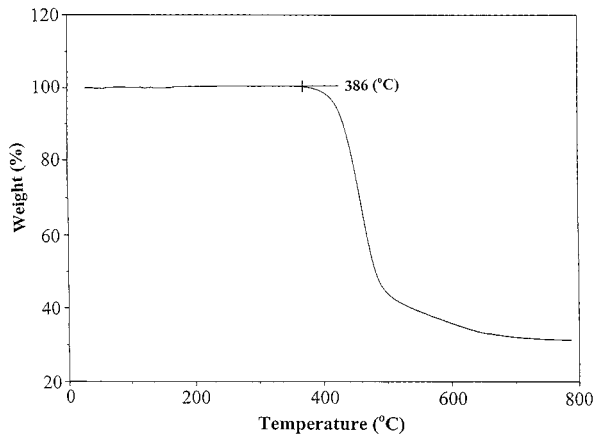

Figure 2. Thermogravimetric analysis of copolymer **II** in nitrogen.

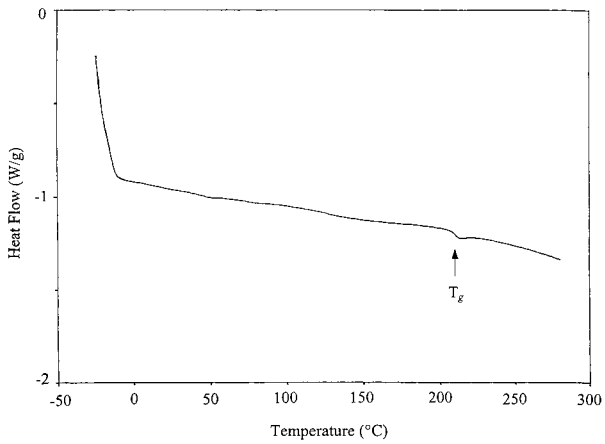

Figure 3. DSC scan for polymer **II** in flowing nitrogen at a heating rate of 20 °C/min.

The DSC results indicate that the polymer possesses a high T_g, which may be an advantage for the PLED device fabrication. It is said that materials with high glass transition temperature as the active emissive layer or charge injecting/transporting layer can provide the device longevity.[19]

The UV−vis absorption and photoluminescence (PL) spectra of the copolymer are depicted in Figure 4. The absorption spectra of both the solution sample and film show two peaks, and the λ_{max} are 318, 426 nm and 329, 426 nm, respectively. The longer wavelength peak in the region of 370−500 nm is attributed to the electron transition of $\pi-\pi^*$ along the conjugated polymer main chain, while the shorter wavelength peak in 250−370 nm originates from the electron transition of the aromatic side chains. It can also be found that the longer wavelength peaks for the solution and film samples are the same. This result indicates that the conformation of the polymer in solution and as films is very similar, which means even the polymer film is in a rather disordered state. The edge absorption for the film sample is 525 nm, which corresponds to a band gap of 2.36 eV. This band gap is smaller than that of another PPV derivative with an oxadiazole pendant (2.48 eV).[5a] Compared to the polymer in ref 5a, the red shift of the maximum absorption should be ascribed to the intro-

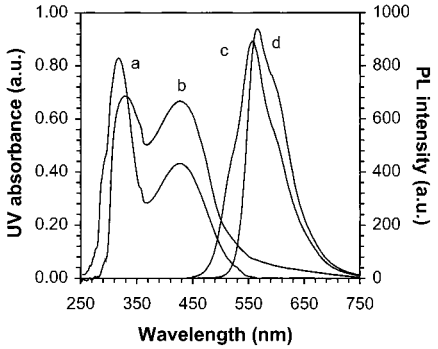

Figure 4. UV−vis spectra (a, b) and photoluminescence spectra (c, d) of the copolymer **II** in solution (a, c) and as films (b, d).

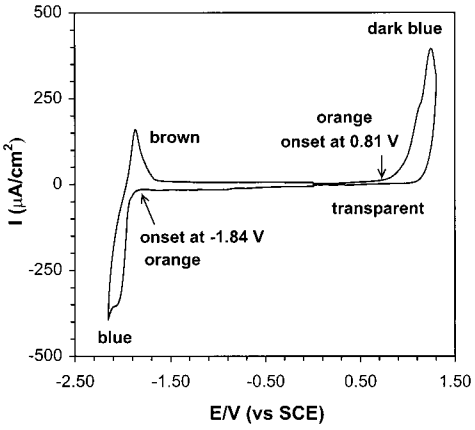

Figure 5. Cyclic voltammogram of copolymer **II** coated on Pt electrodes in acetonitrile containing 0.1 M Bu_4NBF_4 at a scan rate of 20 mV/s; a Pt wire as the counter electrode and Ag/0.1 M $AgNO_3$ in acetonitrile as the reference electrode.

duction of another alkoxy-substituted block on one aspect of electron-donating effect and also due to the improved coplanarity of the polymer main chain. The bulky substituent in polymer **I** or in the polymer[5a] cited herein causes the steric hindrance and will make the phenylene ring or vinylene unit twist; therefore, the π-conjugation will be interrupted. When another block with merely two long alkoxy chains is inserted into the polymer backbone, the bulky side chain interaction will be reduced, and the conjugation of the π electrons along the polymer chain will be enhanced. The emission spectra, which are obtained by excitation at 426 nm, are also quite similar for the solution and film samples. The maximum emission peaks are at 558 and 567 nm, respectively, which correspond to orange-yellow light. The λ_{max} of PL spectrum is intermediate between PPV and dialkoxy-substituted PPVs due to the bulky aromatic groups and alkoxy groups on the two blocks as the side chains, respectively.

Cyclic voltammetry (C−V) was employed to investigate the redox behavior of polymer **II** and to estimate the HOMO and LUMO energy levels of the material.[35] The polymer film dip-coated on a Pt electrode was scanned positively and negatively separately in 0.1 M tetrabutylammonium tetrafluoroborate (Bu_4NBF_4) in anhydrous acetonitrile. Figure 5 depicts the C−V spectra of both p-doping and n-doping processes. During the cathodic scan, the film of polymer **II** exhibits reversible n-doping and dedoping processes. The cathodic peak exhibits at −2.06 V (vs SCE) with corresponding anodic peaks at −1.90 V (vs SCE). The onset potential of the reduction is −1.84 V (vs SCE). The reduction potential is comparable to that of 2-(4-biphenylyl)-5-(4-*tert*-butylphenyl)-1,3,4-oxadiazole (PBD) (−1.95 to −1.94 V vs SCE),[36] and some other polymers containing the oxadiazole unit incorporated into the polymer main chain such as poly(*p*-phenyleneoxadiazole-2,5-diyl) (E^{red} = −1.97 V vs SCE) and poly(pyridine-2,5-diyl-oxadiazole-2,5-diyl) (E^{red} = −2.20 V vs SCE),[31] which are the typical electron-transporting/hole-blocking materials. In our system, although the oxadiazole unit is inserted into the side chain of the copolymer as the electron-withdrawing group, the effect of decreasing the reduction potential is obtained. This can be partly ascribed to the high electron affinity of the oxadiazole unit. Of course, several aromatic rings incorporated into the side chains of the copolymer can increase the delocalization of the π electrons in the ground state, which will make it easy to accept an additional electron so as to have the effect of lowering the reduction potential.[31] The electrochemical reduction of the thin films of the copolymer on Pt is stable during the repeated scanning, and no obvious change of the feature of C−V is observed. The reduction of the copolymer film is accompanied by the change in color from orange to blue and to brown after oxidation.

When a positive sweep potential was applied, an irreversible redox curve was obtained. The prominent anodic peak appeared at 1.25 V (vs SCE), which was accompanied by a shoulder peak at 1.13 V. The two anodic peaks could be attributed to the two different blocks in the copolymer. The onset for the p-doping is determined to be 0.81 V. Along with the oxidation process, the film color changes first from orange to dark blue and then to transparent. From the onset potentials of the reduction and oxidation process, the band gap of the copolymer can be estimated to be 2.65 eV, which is higher than the datum obtained from the edge absorption of UV−vis spectra.

The onset potentials of p-doping and n-doping processes can be utilized to estimate the HOMO and LUMO energy levels of a conjugated polymer. According to the empirical relation obtained by fitting calculations to the experimental data through the valence effective Hamiltonian (VEH) technique, the HOMO and LUMO energy levels can be obtained from the following equations:

$$E_{LUMO} = E^{onset(red)} + 4.4 \text{ eV}$$

$$E_{HOMO} = E^{onset(ox)} + 4.4 \text{ eV}$$

where $E^{onset(ox)}$ and $E^{onset(red)}$ are the onset potentials for the oxidation and reduction processes of a polymer vs SCE, respectively.[37] The LUMO energy of the polymer is thus determined to be 2.56 eV. This value is almost the same as that of some poly(aromatic oxadiazole)s.[31] It implies that the polymer may have similar electron-injection properties with those typical oxadiazole-containing electron-transporting materials when it is used as the emitter in PLEDs. However, the LUMO energy level of 2.56 eV is smaller than that of CN−PPV (3.02 eV). The HOMO energy level can be estimated to be 5.21 eV. This value is lower than that of PPV (5.4 eV).[35] This means that the polymer has better hole injection ability than PPV when it is used in PLEDs. From this preliminary result, a better quantum efficiency can be expected when using this polymer as the emission material for a single-layer PLED due to its

improved electron affinity and better hole injection ability. Further work related to EL performance evaluation is in progress.

Conclusion

A PPV-based homopolymer as well as a copolymer has been successfully synthesized through the Gilch route and Wittig reaction, respectively. The polymers have been introduced an electron-deficient oxadiazole moiety as the side chain so as to enhance the electron affinity. The structural design for the side chain is based on an idea to imitate the structure of PBD, a well-known and widely used electron-transporting material. Among the two polymers, the homopolymer is insoluble due to its too rigid structure while the copolymer can readily dissolve in conventional organic solvents, which makes it proccessable. The copolymer has quite good thermal stability and no decomposition takes place below 386 °C, while DSC analysis reveals that the polymer possesses a T_g higher than 200 °C, which might be a merit for longer device operation when it is used as the emission material. The absorption and fluorescent emission spectra of the polymer indicate that it is an orange-yellow emitting material with a band gap of 2.36 eV. UV−vis spectra show two peaks, which correspond to the $\pi-\pi^*$ transition of conjugated polymer backbone and its side chains. Electrochemical behavior of the copolymer demonstrates that the polymer has similar electron injection ability to PBD and better hole injection ability than PPV. Therefore, a better quantum efficiency can be expected when using this polymer as the emission layer for the single-layer LED device. The optoelectronic properties of the polymer imply that it is a promising material for the PLED application.

References and Notes

(1) Burroughes, J. H.; Bradley, D. D. C.; Brown, A. R.; Marks, R. N.; Mackay, K.; Friend, R. H.; Burn, P. L.; Holmes, A. B. *Nature* **1990**, *347*, 539.

(2) Gustafsson, G.; Cao, Y.; Treacy, G. M.; Klavetter, F.; Colaneri, N.; Heeger, A. J. *Nature* **1992**, *357*, 477.

(3) Greenham, N. C.; Moratti, S. C.; Bradley, D. D. C.; Friend, R. H.; Burn, P. L.; Holmes, A. B. *Nature* **1993**, *365*, 628.

(4) (a) Burn, P. L.; Holmes, A. B.; Kraft, A.; Bradley, D. D. C.; Brown, A. R.; Friend, R. H.; Gymer, R. W. *Nature* **1992,** *356*, 47. (b) Yang, Y.; Pei, Q. *J. Appl. Phys.* **1995,** *77*, 4807. (c) Bettenhausen, J.; Strohriegl, P. *Adv. Mater.* **1996**, *8*, 507. (d) Kraft, A. *Chem. Commun.* **1996,** 77.

(5) (a) Chung, S. J.; Kwon, K. Y.; Lee, S. W.; Jin, J. I.; Lee, C. H.; Lee, C. E.; Park, Y. *Adv. Mater.* **1998**, *10*, 1112. (b) Bao, Z.; Peng, Z.; Galvin, M. E.; Chandross, E. A. *Chem. Mater.* **1998**, *10*, 1201.

(6) (a) Yoshida, M.; Fujii, A.; Ohmori, Y.; Yoshino, K. *Jpn. J. Appl. Phys.* **1996,** *35*, L397. (b) Hamaguchi, M.; Yoshino, K. *Appl. Phys, Lett.* **1996,** *69*, 143. (c) Yoshida, M.; Fujii, A.; Ohmori, Y.; Yoshino, K. *Appl. Phys. Lett.* **1996,** *69*, 734.

(7) (a) Heeger, A. J.; Braun, D. WO-B 92/16023, 1992. (b) Son, S.; Dodabalapur, A.; Lovinger, A. J.; Galvin, M. E. *Science* **1995,** *269*, 376. (c) Hoger, S.; McNamara, J. J.; Schricker, S.; Wudl. F. *Chem. Mater.* **1994,** *6*, 171.

(8) Grem, G.; Leditzky, G.; Ullrich, B.; Leising, G. *Adv. Mater.* **1992,** *4*, 36.

(9) Yang, Y.; Pei, Q.; Heeger, A. J. *J. Appl. Phys.* **1996,** *79*, 934.

(10) Berggren, M.; Inganäs, O.; Gustafsson, G.; Rasmusson, J.; Andersson, M. R.; Hjertberg, T.; Wennerström, O. *Nature* **1994**, *372*, 444.

(11) Andersson, M. R.; Berggren, M.; Inganäs, O.; Gustafsson, G.; Gustafsson-Carlberg, J. C.; Selse, D.; Hjertberg, T.; Wennerström, O. *Macromolecules* **1995**, *28*, 7525.

(12) Wang, Y. Z.; Gebler, D. D.; Lin, L. B.; Blatchford, J. W.; Jessen, S. W.; Wang, H. L.; Epstein, A. J. *Appl. Phys. Lett.* **1996**, *68*, 894.

(13) Wang, Y. Z.; Gebler, D. D.; Fu, D. K.; Swager, T. M.; Epstein, A. J. *Appl. Phys. Lett.* **1997**, *70*, 3215.

(14) Ohmori, Y.; Uchida, M.; Muro, K.; Yoshino, K. *Jpn. J. Appl. Phys.* **1991**, *30*, L1941.

(15) Pei, Q.; Yang,Y. *J. Am. Chem. Soc.* **1996**, *118*, 7416.

(16) Ranger, M.; Rondeau, D.; Leclerc, M. *Macromolecules* **1997**, *30*, 7686.

(17) Wang, C.; Yuan, C.; Wu, H.; Wei, Y. *J. Appl. Phys.* **1995**, *78*, 2679.

(18) (a) Tao, X. T.; Zhang, Y. D.; Wada, T.; Sasabe, H.; Suzuki, H.; Watanabe, T.; Miyata, S. *Adv. Mater.* **1998**, *10*, 226. (b) Lee, J. H.; Aprk, J. W.; Choi, S. W. *Synth. Met.* **1997**, *88*, 31.

(19) (a) Strukelj, M.; Papadimitrakopoulos, F.; Miller, T. M.; Rothberg, L. J. *Science* **1995**, *267*, 1969. (b) Tokito, S.; Tanaka, H.; Noda, K.; Okada, A.; Taga, Y. *Appl. Phys. Lett.* **1997**, *70*, 1929.

(20) (a) Pei, Q.; Yang, Y. *Chem. Mater.* **1995**, *7*, 1568. (b) Li, X. C.; Cacialli, F.; Giles, M.; Gruner, J.; Friend, R. H.; Holmes, A. B.; Moratti, S. C.; Yong, T. M. *Adv. Mater.* **1995**, *7*, 898.

(21) Buchwald, E.; Meier, M.; Karg, S.; Posch, P.; Schmidt, H. W.; Strohriegl, P.; Riess, W.; Schwoerer, M. *Adv. Mater.* **1995**, *7*, 839.

(22) Brown, A. R.; Bradley, D. D. C.; Burroughes, J. H.; Friend, R. H.; Greenham, N. C.; Burn, P. L.; Holmes, A. B.; Kraft, A. *Appl. Phys. Lett.* **1992**, *61*, 2793.

(23) Zhang, C.; Vonseggern, H.; Kraabel, B.; Schmidt, H. W.; Heeger, A. J. *Synth. Met.* **1995**, *72*, 185.

(24) (a) Greenham, N. C.; Friend, R. H. In *Solid State Physics*; Ehrenreich, H., Spaepen, F., Eds.; Academic Press: San Diego, CA 1995; Vol. 49, p 131. (b) Brutting, W.; Berleb, S.; Egerer, G.; Schwoerer, M.; Wehrmann, R.; Elschner, A. *Synth. Met.* **1997**, *91*, 325.

(25) Halls, J. J. M.; Walsh, C. A.; Greenham, N. C.; Marseglia, E. A.; Friend, R. H.; Moratti, S. C.; Holmes, A. B. *Nature* **1995**, *376*, 498.

(26) Yu, W.-L.; Meng, H.; Pei, J.; Lai, Y.-H.; Chua, S.-J.; Huang, W. *Chem. Commun.* **1998**, 1957.

(27) Huang, W.; Yu, W.-L.; Meng, H.; Pei, J.; Li, S. F. Y. *Chem. Mater.* **1998**, *10*, 3340.

(28) Yu, W.-L.; Meng, H.; Pei, J.; Huang, W.; Li, Y.-F.; Heeger, A. J. *Macromolecules* **1998**, *31*, 4838.

(29) Huang, W.; Meng, H.; Yu, W.-L.; Gao, J.; Heeger, A. J. *Adv. Mater.* **1998**, *10*, 593.

(30) Yu, W.-L.; Meng, H.; Pei, J.; Huang, W. *J. Am. Chem. Soc.* **1998**, *120*, 11808.

(31) Janietz, S.; Schulz, B. *Eur. Polym. J.* **1996**, *32*, 465.

(32) Ruiz, J. P.; Dharia, J. R.; Reynolds, J. R.; Buckley, L. J. *Macromolecules* **1992**, *25*, 849.

(33) (a) Yan, M.; Rothberg, L. J.; Papadimitrakopoulos, F.; Galvin, M. E.; Miller, T. M. *Phys. Rev. Lett.* **1994**, *73*, 744. (b) Rothberg, L. J.; Yan, M.; Kwock, E. W.; Miller, T. M.; Galvin, M. E.; Son, S.; Papadimitrakopoulos, F. *IEEE Trans. Electron Dev.* **1997**, *44*, 1258.

(34) Wudl, F.; Hoger, S. US Patent 1997, 5679757.

(35) Cervini, R.; Li, X. C.; Spencer, G. W. C.; Holmes, A. B.; Moratti, S. C.; Friend, R. H. *Synth. Met.* **1997**, *84*, 359.

(36) Janietz, S.; Wedel, A. *Adv. Mater.* **1997**, *9*, 403.

(37) (a) Bredas, J. L.; Silbey, R.; Boudreux, D. S.; Chance, R. R. *J. Am. Chem. Soc.* **1983**, *105*, 6555. (b) deLeeuw, D. M.; Simenon, M. M. J.; Brown, A. B.; Einerhand, R. E. F. *Synth. Met.* **1997**, *87*, 53.

MA981884Y